UTEB #1263586, VOL 00, ISS 00

Geological occurrence, mineralogical characterization, and risk assessment of potentially carcinogenic erionite in Italy

Matteo Giordani, Michele Mattioli, Paolo Ballirano, Alessandro Pacella, Marco Cenni, Matteo Boscardin, and Laura Valentini

QUERY SHEET

This page lists questions we have about your paper. The numbers displayed at left can be found in the text of the paper for reference. In addition, please review your paper as a whole for correctness.

Q1: Au: Please provide missing affiliation (Department)
Q2: Au: References [Bertino et al., 2007; Carbone et al., 2011; Jones, 1968] have been updated. OK?
Q3: Au: Please provide missing [Book title/publisher name/publisher location] for [Bish and Ming, 2001].
Q4: Au: Please provide missing [State/Country] for [Cenni, 2009].
Q5: Au: Please provide missing [State/Country] for [Farrugia, 1999].
Q6: Au: Please cite [Farrugia, 1999] in text or delete reference.
Q7: Au: Please provide missing [State/Country] for [IARC, 1987].
Q8: Au: Please provide missing [publisher name] for [IARC, 1987].
Q9: Au: Please provide missing [State/Country] for [IARC, 1997].
Q10: Au: Please provide missing [publisher name] for [IARC, 1997].
Q11: Au: Please provide missing [State/Country] for [IARC, 2012].
Q12: Au: Please provide missing [publisher name] for [IARC, 2012].
Q13: Au: Please provide missing [State/Country] for [INAIL, 2012].
Q14: Au: Please provide missing [State/Country] for [Muhle et al., 1991].
Q15: Au: Please provide missing [volume number] for [Passaglia and Tagliavini, 1995].
Q16: Au: Please provide missing [volume number] for [Rinaldi, 1976].
Q17: Au: Please provide missing [volume number] for [Sacerdoti, 1996].
Q18: Au: Please provide missing [State/Country] for [Young, 1993].
Q19: Au: Please provide missing [Publisher name] for [Young, 1993].
Q20: Au: Please cite [Young, 1993] in text or delete reference.
Q21: Au: Please provide Table Caption for all the Tables.
Q22: Au: Please provide Figure Caption for all the Figures.
Q23: Au: Please provide significance of "*" with values in Table 3.

TABLE OF CONTENTS LISTING

The table of contents for the journal will list your paper exactly as it appears below:

JOURNAL OF TOXICOLOGY AND ENVIRONMENTAL HEALTH, PART B
2016, VOL. 00, NO. 00, 1–23
http://dx.doi.org/10.1080/10937404.2016.1263586

Taylor & Francis
Taylor & Francis Group

Geological occurrence, mineralogical characterization, and risk assessment of potentially carcinogenic erionite in Italy

Matteo Giordani[a], Michele Mattioli [a], Paolo Ballirano[b,c], Alessandro Pacella[b], Marco Cenni[a], Matteo Boscardin[d], and Laura Valentini[e]

[a]Dipartimento di Scienze Pure e Applicate, Università di Urbino Carlo Bo, Urbino, Italy; [b]Dipartimento di Scienze della Terra, Sapienza Università di Roma, Roma, Italy; [c]Laboratorio Fibre e Particolato Inorganico, Sapienza Università di Roma, Roma, Italy; [d]Museo di Archeologia e Scienze Naturali "G. Zannato", Montecchio Maggiore, VI, Italy; [e]Dipartimento di Scienze Biomolecolari, Università di Urbino Carlo Bo, Urbino, Italy

ABSTRACT

Erionite is a zeolite representing a well-known health hazard. In fact, exposure of humans to its fibers has been unequivocally associated with occurrence of malignant mesothelioma. For this reason, a multi-methodological approach, based upon field investigation, morphological characterization, scanning electron microscopy (SEM)/energy-dispersive spectroscopy (EDS) chemical analysis, and structure refinement through X-ray powder diffraction (XRPD), was applied to different samples of potentially carcinogenic erionite from Northern Italy. The studied crystals have a chemical composition ranging from erionite-Ca to erionite-Na and display variable morphologies, varying from prismatic, through acicular and fibrous, to extremely fibrous asbestiform habits. The fibrous samples were characterized by an unusual preferred partition of aluminum (Al) at tetrahedral site T1 instead of tetrahedral site T2. Further, a mismatch between the a-parameter of erionite-Ca and levyne-Ca that are intergrown in the asbestiform sample was detected. This misfit was coupled to a relevant micro-strain to maintain structure coherency at the boundary. Erionite occurs in 65% of the investigated sites, with an estimated quantity of 10 to 40 vol% of the associated minerals. The presence of this mineral is of concern for risk to human health, especially if one considers the vast number of quarries and mining-related activities that are operating in the zeolite host rocks. The discovery of fibrous and asbestiform erionite in Northern Italy suggests the need for a detailed risk assessment in all Italian areas showing the same potential hazard, with specific studies such as a quantification of the potentially respirable airborne fibers and targeted epidemiological surveillance.

Introduction

A few decades ago, an epidemic of malignant mesothelioma (MM) was recognized in some villages of Cappadocia, Central Anatolia, Turkey (Artvinli and Baris 1979; Baris et al. 1978, 1979). According to mineralogical studies and analysis of lung content, this epidemic was unequivocally linked to the occurrence of fibers of erionite of inhalable size in the region's bedrock (Baris et al. 1987, 2011; Carbone et al. 2007; Dogan et al. 2006; Emri et al. 2002; Metintas, Hillerdal, and Metintas 1999). Further, experimental studies demonstrated that fibrous erionite of inhalable size is more carcinogenic and more active than chrysotile and crocidolite asbestos in increasing the incidence of mesothelioma (Andujar et al. 2016; Bertino et al. 2007; Coffin, Cook, and Creason 1992; Croce et al. 2013; Crovella et al. 2016; Davis et al. 1991; de Assis, Locatelli, and Isoldi 2014; Dogan 2012; Hill, Edwards, and Carthew 1990; Hillegass et al. 2013; Pollastri et al. 2014; Wagner et al. 1985; Zebedeo et al. 2014). For these reasons, and according to epidemiological data (Baris et al. 1978, 1979, 1987; Baumann and Carbone 2016; Carbone et al. 2007; Carbone and Yang 2012; Demirer et al. 2015; Kliment, Clemens, and Oury 2009; Kokturk et al. 2005; Temel and Gündogdu 1996), erionite has been classified as carcinogenic mineral for human

CONTACT Michele Mattioli michele.mattioli@uniurb.it University of Urbino Carlo Bo, Department of Pure and Applied Sciences, Scientific Campus E. Mattei - Via Ca' Le Suore 2/4, 61029 URBINO, Italy.

Color versions of one or more of the figures in the article can be found online at www.tandfonline.com/uteb.
Supplementary material for this article can be accessed on the publisher's website.

health and referred to as a Class 1 carcinogen by the International Agency for Research on Cancer since 1987, and at present, it is categorized as the most carcinogenic mineral (IARC 1987, 2012).

Despite the fact that erionite was considered for a long time as a relatively uncommon mineral (Bish and Ming 2001; Passaglia and Galli 1974), this fiber was recently found in many localities worldwide (Supplementary Material, Table S1). In Italy, the occurrence of erionite was reported in some areas of Sardinia and Veneto regions (Giovagnoli and Boscardin 1979; Passaglia and Galli 1974; Passaglia and Tagliavini 1995; Pongiluppi, Passaglia, and Galli 1974). Although it is known that this fiber is highly dangerous, a systematic investigation and mapping of its distribution are still missing for the Italian area, and little attention has been devoted to examining the potential adverse health risks attributed to environmental exposures. Recently, new occurrences of erionite were detected in volcanic rocks of NE Italy (Giordani et al. 2016; Mattioli, Cenni, and Passaglia 2016a), suggesting that this hazardous mineral may be more widespread than currently presumed, especially in other areas with suitable geological characteristics.

The aim of the present investigation was to provide a field description and detailed mineralogical characterization of selected samples of potentially carcinogenic fibrous erionite recently discovered in the Lessini Mountains (Veneto region, NE Italy). Scanning electron microscopy (SEM) with energy-dispersive spectroscopy (SEM-EDS) and X-ray powder diffraction (XRPD) data were combined and integrated, in order to characterize from a crystal chemical and structural point of view this health-threatening mineral. Another aim of this study was to review the locations in which erionite fibers were detected and described in Italy, trying to recognize the other geological settings where it may potentially occur. This information represents a useful basis for future studies by geological, mining, and medical investigators, in particular, aimed at examining potential correlations between geological occurrences and epidemiological data of the distribution of pulmonary diseases typically related to erionite exposure.

Mineralogy

Erionite was first identified near Durkee, Oregon, (USA) by Eakle (1898) who described the "woolly" variety (the erionite name derives from the Greek word for wool) that occurs at the type locality consisting of white, woolly-like fibers. Erionite is a zeolite belonging to the ABC-6 family (Gottardi and Galli 1985). It is hexagonal, space group $P6_3/mmc$, unit-cell parameters a = 13.19–13.34 Å, c = 15.04–15.22 Å (Alberti et al. 1997; Bish and Ming 2001; Cametti et al. 2013; Deer et al. 2004; Gualtieri et al. 1998; Staples and Gard 1959), and average chemical formula $Na_2K_2Ca_3[Al_{10}Si_{26}O_{72}]30H_2O$. Its framework consists of $(Si,Al)O_4$ tetrahedra linked together to form single or double layers of six-membered rings, whose stacking along the z-axis, following the AABAAC sequence, produces three types of cages: a double six-membered [D6 R] ring (empty), a cancrinite [CAN] cage (preferred by K), and an erionite [ERI] cavity hosting Ca, Na, Mg, and additional K (Alberti et al. 1997; Ballirano et al. 2009; Bish and Ming 2001; Cametti et al. 2013; Deer et al. 2004; Gottardi and Galli 1985; Passaglia, Artioli, and Gualtieri 1998).

Previously, erionite was described as a single mineral species (Gude and Sheppard 1981; Passaglia and Sheppard 2001; Sheppard and Gude 1969), while at present it is classified as a series, owing to a significant chemical variability, consisting of three different species, erionite-K, erionite-Ca, and erionite-Na, depending upon the most abundant extra-framework (EF) cation (Ballirano et al. 2009; Coombs et al. 1997; Dogan and Dogan 2008; Dogan, Dogan, and Hoskins 2008).

Erionite is often misidentified with offretite, a closely related zeolite (AAB stacking sequence). The distinction between these species may be difficult because of their physical, chemical, and structural similarities, and because of the possibility of their intergrowth within a single crystal (Gualtieri et al. 1998; Passaglia, Artioli, and Gualtieri 1998). The most significant discrimination between erionite and offretite is based upon the Mg/(Ca + Na) cation ratio. Under such aspect, offretite displays values close to 1, whereas those of erionite do not exceed 0.3 (Passaglia, Artioli, and Gualtieri 1998). Among the minerals that might be found in intimate association with erionite, levyne, another ABC-6 zeolite (AABCCABBC stacking sequence), is the most relevant as it generally forms an epitaxial intergrowth, giving rise to an

alteration of levyne-erionite layers (Giordani et al. 2016; Passaglia and Galli 1974; Rinaldi 1976; Wise and Tschernich 1976).

Erionite geology

Erionite, as well as many other zeolites, often has hydrothermal origin and is related to the presence of fluids arising and/or heated from below (Wylie and Candela 2015). Under favorable conditions, these hydrothermal solutions can be able to induce crystallizations in the empty spaces of traprocks, especially in the case of high-vesiculated tuff and lavas (Bish and Ming 2001; Gottardi and Galli 1985; Passaglia, Artioli, and Gualtieri 1998). However, Bish and Ming (2001) recognized that huge quantities of zeolites also occur as low-temperature, low-pressure alteration products of pyroclastic material, and that many of the zeolites filling vugs and cavities of basalts are diagenetic in origin, being precipitated directly from ground water percolating through the rock mass.

In recent years, erionite has been recognized as important mineral in low-grade metamorphic and in a variety of sedimentary rocks of different lithology, age, and depositional environments. Erionite of sedimentary origin might originate from a variety of precursor materials including volcanic glass and aluminosilicate minerals that react to form zeolites by dissolution–precipitation processes (Bish and Ming 2001; Deer et al. 2004; Gottardi and Galli 1985; Passaglia, Artioli, and Gualtieri 1998). Erionite from Cappadocia, Turkey, appears to have formed in this manner where huge deposits of volcanic tuffs have undergone, after deposition, a series of geochemical changes including dissolution of volcanic glass and re-precipitation of smectite, followed by widespread crystallization of erionite in the pore spaces. Most erionites in sedimentary rocks occur as microscopic or submicroscopic crystals being therefore hardly recognizable in the hand specimen. However, deposits of this type are voluminous and display significant geological relevance and economic/toxicologic potential.

Erionite is just one among several natural zeolites commonly occurring with fibrous habit and is by far the most studied from the toxicological point of view. However, attention is in the scientific community to determine whether fibers of zeolites such as mordenite, clinoptilolite, phillipsite, offretite, thomsonite, mesolite, scolecite, natrolite, paranatrolite, gonnardite, mazzite, roggianite, and perlialite may also be hazardous to human health. As reported in the IARC Monograph (1997), there is inadequate evidence in humans for carcinogenicity of zeolites other than erionite, and there is inadequate evidence in experimental animals for carcinogenicity attributed to clinoptilolite, phillipsite, and mordenite. Nevertheless, recent investigations on the surface properties of selected fibers of zeolites revealed that the availability of surface sites for adsorption and interacting ability is significant not only for erionite, but also for fibrous offretite and scolecite (Mattioli et al. 2016b). Considering that these properties may be related to carcinogenic potential, a great necessity emerges to increase the available information on these minerals, given the abundant occurrence of zeolite deposits worldwide.

Erionite health risks

It is well known that small particles, especially those with fibrous morphology, generate biological processes leading to toxicity and carcinogenicity inside the lungs (Andujar et al, 2016; Aust, Cook, and Dodson 2011; Coffin, Cook, and Creason 1992; Cook, Palekar, and Coffin 1982; Crovella et al. 2016; Davis et al. 1991; Fubini 2001; Larson et al. 2016; Lemen 2016; Millette 2006; Pott et al. 1987; Stanton et al. 1981; Wagner et al. 1985). One of the most important factors that define the adverse health severity of a mineral fiber is its breathability, which depends on the size including length, diameter, and relative ratio and the aerodynamic equivalent diameter (Aust, Cook, and Dodson 2011; Boulanger et al. 2014; Dodson, Atkinson, and Levin 2003; Lee 1985; Millette 2006, 2015; Oberdörster, Oberdörster, and Oberdörster 2005; Pott et al. 1987; Stanton et al. 1981; Wylie and Candela 2015). The fibers biopersistence is also an important factor for their toxicity and carcinogenicity (Fubini 2001; Hesterberg et al. 1998; Maxim et al. 2006). It was postulated that a fiber with critical dimensions may be carcinogenic if sufficiently durable to remain

chemically and physically intact in lung tissue (Muhle, Bellmann, and Pott 1991; Oberdörster, Oberdörster, and Oberdörster 2005). The fibers biopersistence is also related to their chemical composition, with some elements potentially playing a key role to determine carcinogenicity such as the presence of iron (Ballirano et al. 2015; Bonneau, Malard, and Pezerat 1986; Crovella et al. 2016; Fubini 2001; Gazzano et al. 2005; Wiseman and Halliwell 1996). Further, trace elements content, including As, Be, or Pb, and some rare earth elements, may also play a role in fiber toxicity (Bloise et al. 2016).

Other features such as specific surface area, interacting capability, durability, structure, net charge, and microtopography might also act as important factors in particle-induced toxicity and carcinogenicity (Hochella 1993; Lippmann 1988; Mattioli et al. 2016b; Oberdörster, Oberdörster, and Oberdörster 2005). It is relevant to note that these features are the same for a given mineral species regardless of the morphological habit. For this reason, nonfibrous particles released from erionite with prismatic habit might also be considered potentially able to elicit reactions in the respiratory system. Moreover, the potential for reactivity is further enhanced for some dusts like erionite because of inherent pores/voids, which create notable surface areas for reactions to occur in a biosystem. In addition, fibrils originating by splitting of fibers may display different mechanical behaviors such as brittleness or flexibility, and this feature represents a critical factor in the assessment of the hazard.

Much of the scientific knowledge regarding toxicity and carcinogenicity of fibrous particles arise from studies carried out on asbestos, certainly the most studied mineral fibers. However, in recent years the number of studies devoted to erionite fibers has significantly increased, shedding new light on the toxicology of fibrous particles. Most of the investigations focused on the Cappadocian emergency following observation of a high mortality rate from MM in the local population (Carbone et al. 2007; Dogan 2003). Recently, targeted epidemiological studies were performed in other sites of the world, with the aim of clarifying whether high incidences of typical asbestos-related lung diseases are linked to the natural presence of erionite fibers. Within a few years, deaths attributed to inhalation of erionite fibers were confirmed in Turkey (Carbone et al. 2011; Dogan et al. 2006), USA (Carbone et al. 2011; Saini-Eidukat and Triplet 2014), Mexico (Ortega-Guerrero et al. 2015), and possibly Iran (Ilgren, Kazemian, and Hoskins 2015). Notwithstanding the growing interest in this particular zeolite and important findings noted regarding the mechanisms underlying carcinogenesis and potential genetic predispositions (Ballirano and Cametti 2015; Ballirano et al. 2015; Carbone and Yang 2012; Hillegass et al. 2013; Lemen 2016; Metintas et al. 2010; Pollastri et al. 2015), the precise sequence of events ranging from deposition of fibers in the human respiratory tract to production of related diseases has not been fully clarified.

Field description and materials

The studied samples are from the Tertiary basalts of Northern Italy (Figure 1), where a thick sequence of lava flows of Veneto Province extensively crops out (Beccaluva et al. 2007; Bonadiman et al. 2001; De Vecchi and Sedea 1995; Milani, Beccaluva, and Coltorti 1999). Whereas the dominant magmatism in the western side of the Northern Apennines during the Tertiary is of subduction-related type (Mattioli et al. 2012), an extensional-related volcanic activity developed in the eastern side of the South Alpine foreland, with the greatest part of the eruptions taking place in submarine environments. Several magmatic pulses occurred between the Late Paleocene and Miocene periods, all of which were of a short duration and separated by periods of magmatic inactivity during which shallow-water carbonate sedimentation occurred (De Vecchi and Sedea 1995).

The Tertiary basalts of the Veneto Province are well known to be suitable host rocks for the development of secondary mineral associations (Cenni 2009; Mattioli, Cenni, and Passaglia 2016a). These secondary mineral assemblages that develop within vesicles and veins are mainly concentrated at the bottom and at the top of each basaltic lava flow. The lower level consists of a thin (up to 30 cm thick), discontinuous, vesicular interval with vesicles of less than 10 vol%, ranging from 1 to 5 cm in diameter. The upper level is

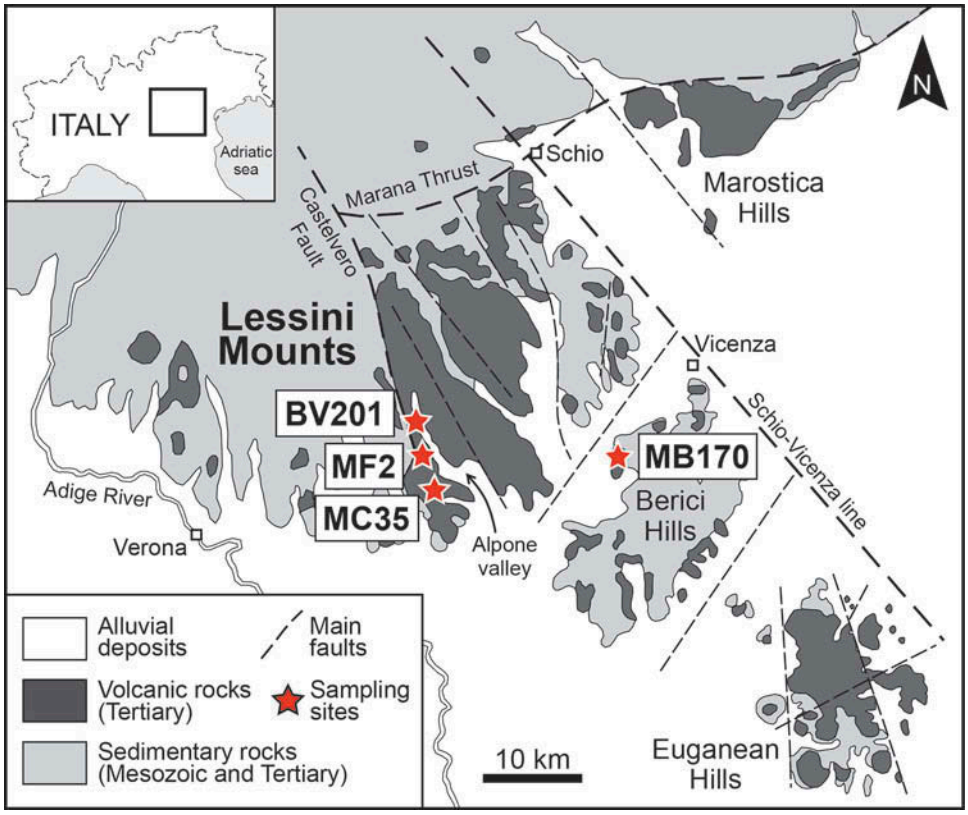

Q22 **Figure 1.**

characterized by altered facies with a huge quantity of vesicles and important concentrations of secondary minerals. At the top of this level, which is 5 to 10 m thick, the vesicularity is approximately 40 vol%, with vesicle diameters from 0.1 to 1 cm, whereas at the base of the upper zone the diameters of the vesicles increase to up to 20 cm and the associated porosity is in the range 5–10 vol% (Mattioli, Cenni, and Passaglia 2016a). Secondary minerals from veins and vesicles were investigated during several field trips. More than one thousand vesicles were studied in the field, approximately 300 of which were sampled and analyzed for identification of secondary minerals. Locations, geographic coordinates, assemblages of secondary minerals, and estimated amounts of erionite are summarized in Table 1.

The secondary phases are mainly zeolites and clay minerals, which represent approximately 90 vol% of total secondary minerals; other silicates (apophyllite, gyrolite, prehnite, pectolite) are rare, as are oxides (quartz) and carbonates (calcite, aragonite). Clay minerals, which form botryoidal aggregates, are generally the first minerals that precipitated along the walls, whereas the core of the vesicles commonly contains well-shaped zeolites. The thickness of the coating is generally less than 0.5 mm, while the zeolite crystals range in size from <1 mm to 1 cm. Among zeolites that are normally the last phases to crystallize, typical vesicle infillings consist of, in order of abundance, chabazite, phillipsite–harmotome, analcime, natrolite, gmelinite, and offretite. Heulandite, stilbite, and erionite are less common, whereas willhendersonite and yugawaralite are rare.

Frequently, several species are present within the same vesicle, even if only one or two of these minerals are detected. The occurrence of different zeolite species and their frequency in the studied rocks is nonhomogeneous, and their associations may be significantly different on both the outcrop and sample scale, showing a variability that might be in the order of a few centimeter. By comparing all of the detailed systematic observations of the assemblages of the main secondary minerals (zeolites and clay minerals), it is apparent that erionite

is present in 65% of the investigated outcrops, with an estimated amount varying from 10 to 40 vol% of total secondary minerals (Table 1).

From the entire suite, four representative samples of erionite were investigated in this study. The four samples were selected on the basis of the main morphological types observed for all erionite occurrences in this area: (1) prismatic crystals with a solid appearance (MC35); (2) acicular crystals with rigid behavior (MF2); (3) acicular to fibrous crystals with rigid to flexible mechanical behavior (MB170); and (4) extremely fibrous with flexible, hair-like appearance (BV201). Morphometric and preliminary chemical data of MF2 and BV201 samples were reported in Giordani et al. (2016). In this investigation, the mineralogical characterization was completed and data integrated with those of the new samples MC35 and MB170, in order to present a picture as comprehensive as possible of the distribution and types of erionite in Italy.

Analytical methods

Scanning electron microscopy

The morphological investigation was carried out at the University of Urbino Carlo Bo using a SEM FEI Quanta 200 FEG environmental scanning electron microscope (ESEM) equipped with an energy-dispersive X-ray spectrometer (EDAX) for semiquantitative chemical analyses. The microchemical composition was determined at the Dipartimento di Scienze della Terra, Sapienza Università di Roma, using a SEM FEI Quanta 400 equipped with an EDS system. Operating conditions were 15 kV accelerating voltage, 11 mm working distance, 0° tilt angle, and 1 µm beam diameter. Chemical data were collected at 30 analytical points. The final crystal chemical formula was calculated, after renormalization of chemical analyses hypothesizing a water content of 18.5 wt. % (corresponding to approximately 30 atoms per formula unit, *apfu*), on the basis of 36 (Si+Al) *apfu*. As previously suggested (Goldstein et al. 1992; Pacella, Ballirano, and Cametti 2016; Reed 1993; Sweatman and Long 1969), in order to minimize the alkali metal migration, chemical data were acquired using a low counting time (up to

Q21

Table 1.

Locality	Latitude	Longitude	Altitude (m a.s.l.)	Mineral association	Erionite (vol. %)
Cercene Mt.	45.430677	11.257841	159	CHA + OFF + CM	-
Foscarino Mt.	45.439427	11.258779	296	PHI/HAR + **ERI** + OFF + CM	35
Colombara	45.426723	11.277245	140	PHI/HAR + CHA + OFF + **ERI** + CM	10
Fittà	45.453548	11.253994	281	GME + PHI/HAR + **ERI** + OFF + CM	15
Gambaretti	45.501002	11.232667	213	CHA + GME + CM	-
Calvarina Mt.	45.490955	11.269361	280	NAT + ANA + **ERI** + OFF + CM	20
Chiereghini Valley	45.549751	11.219361	285	PHI/HAR + NAT + OFF + CM	-
S.Giovanni Ilarione	45.521057	11.236276	194	ANA + **ERI** + OFF + PHI/HAR + CM	35
Beltrami	45.525522	11.229305	253	PHI/HAR + CHA + OFF + CM	-
Bagattei	45.551624	11.218733	329	PHI/HAR + **ERI** + OFF + YUG + CM	40
Contrada Moretti	45.553182	11.218772	312	CHA + WHI + CM	-
Soave	45.419776	11.247955	50	OFF + **ERI** + GYR + PRE + CM	35
Roncà	45.480646	11.288877	80	ANA + OFF + PHI/HAR + CM	-
Prun	45.577982	10.951481	541	CHA + OFF + **ERI** + CM	20
S. Cristina	45.581039	10.940663	683	PHI/HAR + CHA + **ERI** + OFF + CM	15
Mont. Maggiore	45.493091	11.469650	150	PHI/HAR + CHA + **ERI** + CM	30

10 sec) and a raster scan mode to reduce the temperature increase. The reliability of the chemical analysis used to classify the erionite samples was evaluated by using the charge balance error formula (E%: Passaglia 1970; Passaglia, Artioli, and Gualtieri 1998), the Mg-content (Dogan and Dogan 2008; Dogan, Dogan, and Hoskins 2008), and K-content tests (Cametti et al. 2013). Chemical analyses of zeolites are considered to be reliable if the balance error (E%) is within ±10%.

To evaluate the quality of the SEM-EDS microchemical data, two samples (BV201 and MF2) were also investigated by electron microprobe analysis (EMPA). Pure crystals from these samples were prepared embedding a fraction of fibers in epoxy resin. Compositions were determined at the Istituto di Geoscienze e Georisorse, CNR, Padua, using a Cameca SX50 EMPA equipped with wavelength-dispersive spectrometry (WDS). According to the recommended protocol for the quantitative determination of zeolite compositions by EMPA (Campbell et al. 2016), the following conditions were used: reduced counting time (up to 10 sec), beam diameter 20 μm, accelerating voltage 15 kV, low beam current, and element prioritizing with the spectrometer configuration. Silicates, oxides, and pure elements were used as standards; analytical errors are 1–2% rel. and 3–5% rel. for major and minor elements, respectively. Comparing the compositions of the duplicate samples, no relevant differences between the two datasets were observed, indicating the full reliability of the chemical data obtained by the SEM-EDS technique.

X-ray powder diffraction

XRPD data were collected only for samples BV201 and MB170 owing to their fibrous habit and corresponding potential toxicity for humans. Bundles of fibers were selected under a binocular microscope and reduced to powder using an agate mortar and pestle that were loaded into 0.7 mm diameter SiO_2 glass capillaries. Data from XRPD were collected in transmission mode using a D8 advance diffractometer (Bruker AXS, Karlsruhe, Germany) operating in θ/θ geometry. The instrument is fitted with focusing Göbel mirrors on the incident beam, Soller slits on both incident and (radial) diffracted beams, and a PSD VÅNTEC-1 detector. Preliminary diffraction patterns indicated the occurrence of relevant amounts of levyne-Ca (BV201) and minor calcite and barite (MB170). Structure refinements were carried out by the Rietveld method using TOPAS v.4.2 (Bruker AXS, 2009) and modeling the peak shape by fundamental parameters approach (FPA). Owing to the relatively similar chemical composition, the selected starting structural model of erionite was taken from Alberti et al. (1997). Structural data of levyne-Ca were taken from Sacerdoti (1996), whereas those of barite and calcite from Jacobsen et al. (1998) and Ballirano (2011), respectively. The same Rietveld refinement procedure used by the present research group was adopted in several structure refinements of erionite fibers (Ballirano et al. 2009; Ballirano and Cametti 2012). Absorption correction was performed following the procedure of Sabine et al. (1998), and the occurrence of preferred orientation was modeled by spherical harmonics selecting the number of terms to be employed according to the procedure devised by Ballirano (2003). In the case of sample MB170, the refinement was performed using the ellipsoid model of Katerinopoulou, Balic-Zunic, and Lundegaard (2012) describing the diffraction-vector dependent broadening of diffraction maxima. Miscellaneous data of the refinements are listed in Table 2. Rietveld plots of both samples are shown in Figure 2.

Morphology

The main morphological features of the investigated erionites are illustrated in Figure 3.

In the MC35 sample, erionite commonly occurs as elongated, prismatic crystals having a length of about 100–500 μm and a diameter ranging from 10 to 50 μm (Figure 3a). SEM images show that some crystals possess well-formed hexagonal cross sections, while other crystals exhibit irregular morphologies. Much of erionite occurs in radial aggregates or spherulites up to a millimeter in size. More rarely, erionite occurs in stubby bundles of 5–80 μm in length, each of them consisting of tens to hundreds of individual crystals. In this sample, all crystals display a solid appearance and a rigid behavior and no fibrous elements detected.

Table 2.

Instrument	Bruker AXS D8 Advance	
Radiation	CuKα	
Primary and secondary radius (mm)	250	
Detector	PSD VÅNTEC-1	
Sample mount	Rotating capillary (60 r/min)	
Incident beam optics	60 mm multilayer (Göbel) focussing X-ray mirror	
Detector window (°)	6	
Divergence slits (°)	0.3	
Soller slits	Primary beam (2.3°); diffracted beam (radial)	
	BV201	MB170
2θ range (°)	6–145	
Step size (°2θ)	0.022	
Counting time (s)	10	
a (Å)	13.34082(18)	13.31490(13)
c (Å)	15.1229(3)	15.09267(19)
Volume (Å^3)	2330.94(8)	2317.25(5)
c/*a*	1.1342	1.1335
R_{Bragg} (%)	0.356	0.966
R_p (%)	1.445	1.729
R_{wp} (%)	1.877	2.329
GoF	1.714	3.645
Weighted DWd	0.758	0.237
Micro-strain ε_0	0.0736(17)	0.0445(17)
L_{vol} (nm)	72.3(9)	–
r_a (nm)	–	576(9)
r_c (nm)	–	567(11)

In the MF2 sample, erionite is present as single, acicular crystals with diameter of approximately 5 μm and length up to 150 μm demonstrating hexagonal section, or as discrete aggregates of several crystals generally radiating from a central point, joined to form packets of larger size (about 50 μm), where the hexagonal symmetry of each crystal is still recognizable (Figure 3b). Based on SEM observations, the well-developed hexagonal section is present only in the terminations of crystals, consisting of perfect hexagonal prisms of about 15 μm in diameter and 10–20 μm in length. In contrast, the main body of the crystals is thinner (diameter approximately 5 μm) and loss of any reference to the hexagonal basal section. The short hexagonal prisms forming the termination of the crystals show a solid appearance, whereas the main body tends to split up into a great number of fibrils with rigid behavior, partially or totally separated from the main crystal body (Giordani et al. 2016). The MF2 sample displays a marked tendency to subdivide into fibers and fibrils with rigid behavior, which are characterized by variable length and diameter. Regarding the length, the majority of the fibers demonstrate a size generally up to approximately 30 μm, rarely longer, while, in terms of diameter, these fibrils are commonly thinner than approximately 1.5 μm.

In the MB170 sample, erionite occurs as acicular to fibrous crystals always grouped in radial aggregates forming spherules up to one millimeter in size (Figure 3c). The acicular crystals possess dimensions up to some hundreds of millimeter in terms of length and up to approximately 10 μm in diameter. At higher magnification, the spherules and prisms that compose them appear as constituted by bundles of rigid fibers of small diameter, generally less than a few millimeter (Figure 3d). Moreover, whenever fractures and discontinuities occur in these bundles, the presence of a large number of small fibrils was noted with rigid to flexible behavior, with length ranging up to approximately 30 μm and small diameter, consistently smaller than 1 μm.

The BV201 sample consists of two mineralogical species, erionite and levyne, which are grown in intimate association (Figure 3e). This particular intergrowth was previously reported in the Italian area, particularly in Sardinia (Passaglia and Galli 1974) and in the Lessini

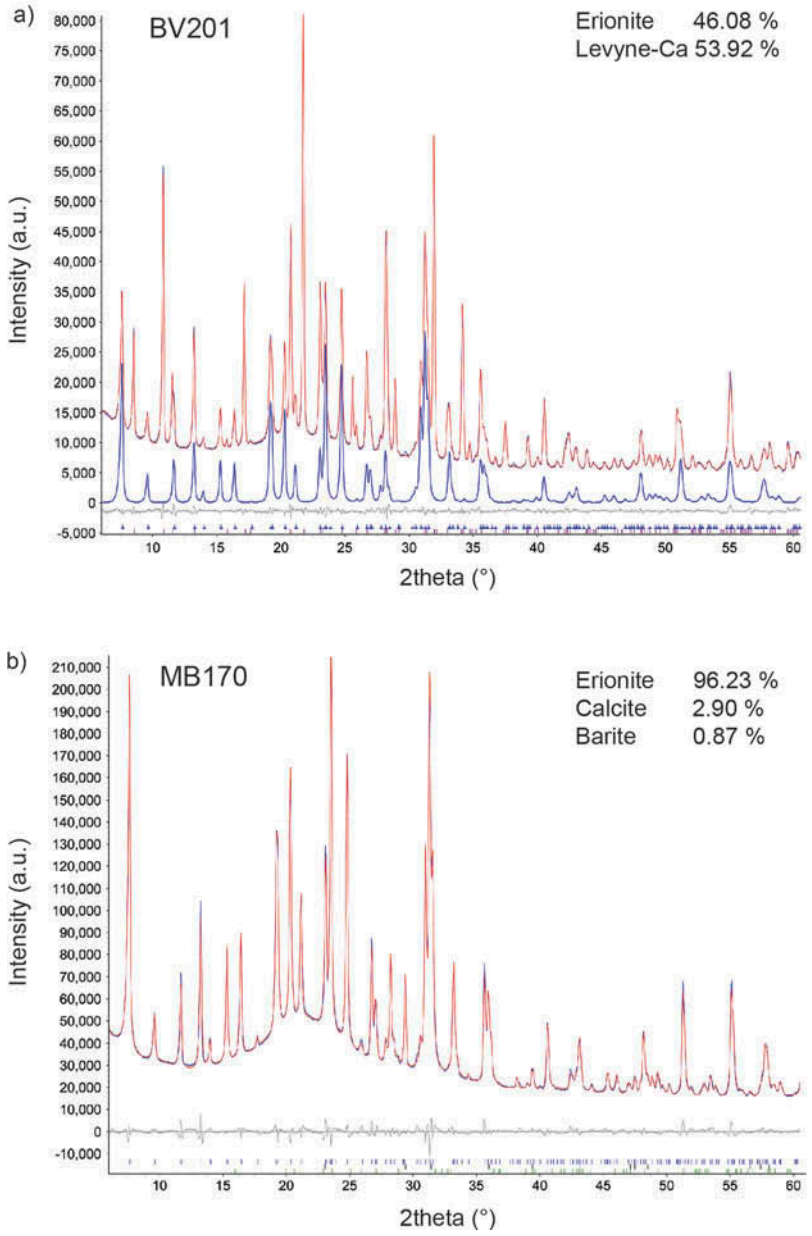

Figure 2.

Mounts (Giordani et al. 2016). In BV201 sample, levyne displays a highly tabular habit with hexagonal section and millimeter size, while erionite grows up normally to the levyne surfaces, forming a typical erionite-levyne-erionite sequence (ELE), which may also be repeated several times forming a "sandwich-like" morphology. In this sample, erionite is characterized by an extremely fibrous habit which consists of flexible fibers grouped in bundles of a few tens of millimeter in diameter and variable length up to approximately 100 µm (Figure 3f). These bundles are consistently prone to separate in a myriad of thin fibers and fibrils of variable size in terms of length (from approximately 5 to 85 µm, main mode 40–60 µm), but homogeneous in terms of diameter, which is <0.3 µm. In this sample, erionite demonstrated the typical woolly aspect of the holotype from Durkee, Oregon (Eakle 1898; Staples and Gard 1959).

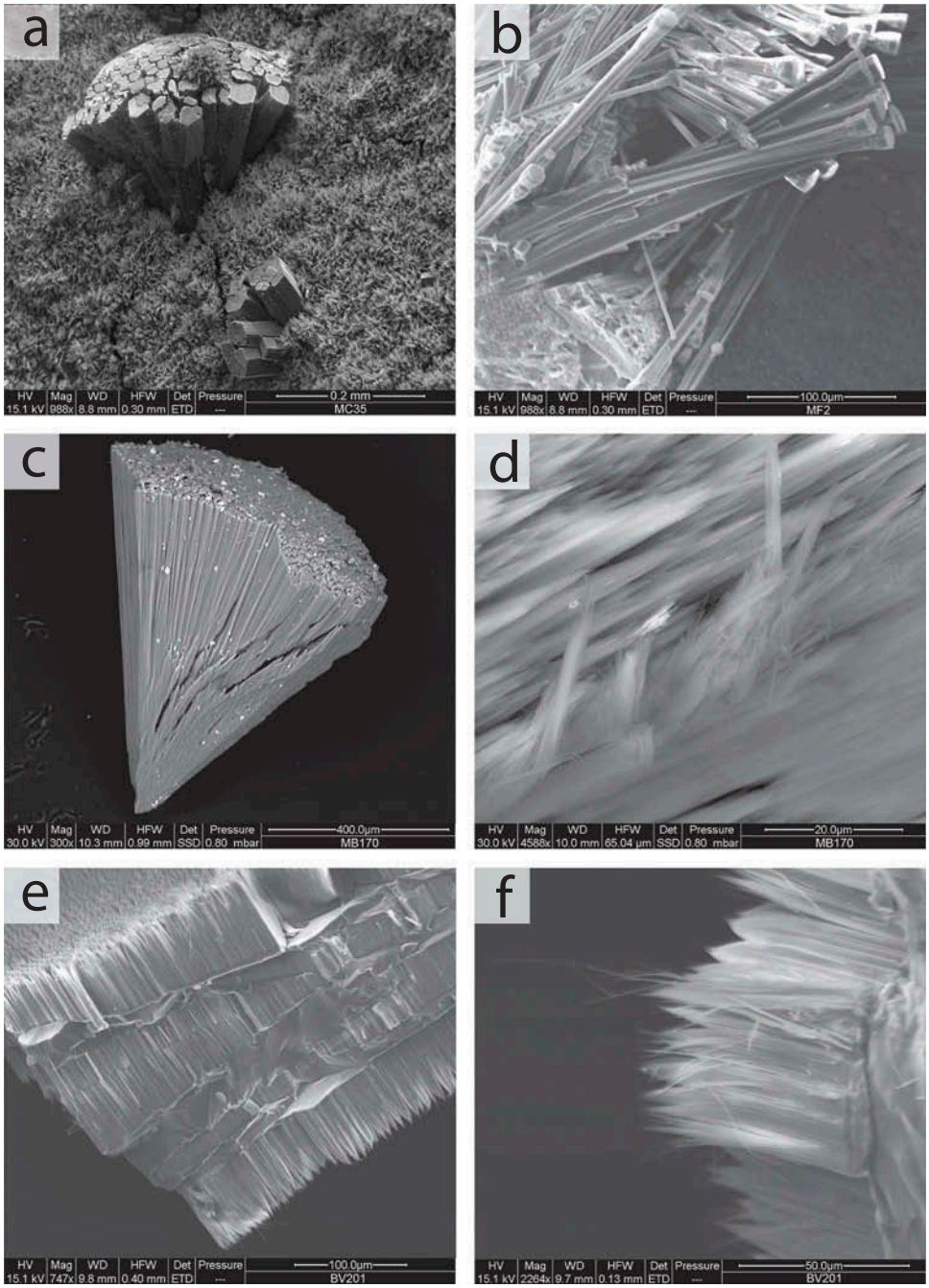

Figure 3.

Chemistry

The point analyses of the samples are highly consistent, showing a variation of major elements within 2–3%, indicating a high degree of chemical homogeneity of each sample. The chemical data of the investigated samples (i.e., analyses passing the quality checks described in analytical methods) are presented in Table 3 and depicted diagrammatically in Figure 4. The prismatic erionite from MC35 has an average chemical formula $(Ca_{2.80}K_{2.29}Na_{1.35}Mg_{0.26})[Al_{10.09}Si_{25.91}O_{72}]\cdot 30.23H_2O$ and classified as erionite-Ca (Figure 4). Ca^{2+} is generally the prevailing EF cation with a content ranging from 2.12 to 3.51 *apfu*, but the amount of K^+ and Na^+ is also high: 2.04–2.51 *apfu* and 0.29–2.62 *apfu*, respectively. In contrast, the Mg^{2+} content is low, 0.11–0.48 *apfu*, leading to a Mg/(Ca+Na) ratio, which is considered the most significant parameter for the distinction between erionite and offretite, of 0.06 (range 0.03–

Q23

Table 3.

	BV201		MF2		MB170		MC35	
Sample	average *N = 15*	σ	average *N = 7*	σ	average *N = 10*	σ	average *N = 10*	σ
SiO_2	52.52	0.71	56.71	1.18	55.43	0.38	53.15	0.66
Al_2O_3	17.97	0.56	15.35	0.88	15.87	0.23	17.54	0.69
MgO	0.35	0.19	0.39	0.24	0.46	0.10	0.36	0.21
CaO	6.70	0.49	3.07	0.52	5.15	0.35	5.35	1.11
Na_2O	0.40	0.27	2.59	0.19	0.49	0.11	1.42	0.89
K_2O	3.54	0.37	3.38	0.23	4.10	0.27	3.68	0.26
H_2O	18.50*	–	18.50*	–	18.50*	–	18.50*	–
Total	81.50	–	81.50	–	81.50	–	81.50	–
Si	25.65	0.33	27.28	0.52	26.91	0.12	25.91	0.38
Al	10.35	0.33	8.72	0.52	9.09	0.12	10.09	0.38
☒*T*	*36.00*	–	*36.00*	–	*36.00*	–	*36.00*	–
Mg	0.26	0.14	0.28	0.17	0.33	0.07	0.26	0.15
Ca	3.51	0.26	1.59	0.28	2.77	0.23	2.80	0.58
Na	0.39	0.26	2.43	0.18	0.46	0.10	1.35	0.85
K	2.21	0.23	2.08	0.14	2.44	0.19	2.29	0.17
H_2O	30.23	0.08	29.90	0.14	30.02	0.17	30.23	0.12
R	0.713	–	0.758	–	0.748	–	0.720	–
E%	2.20	3.53	5.56	3.07	0.64	4.62	3.30	5.06

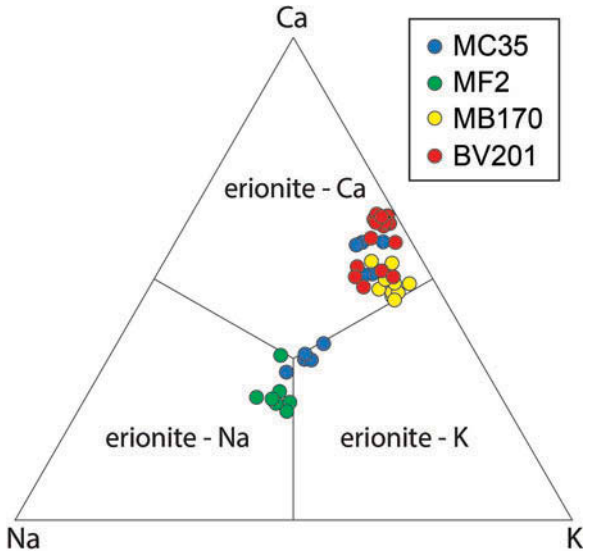

Figure 4.

0.11). However, if one examines the data in more detail, it may be noted that the chemical compositions of the analyzed crystals define two distinct fields in the Figure 4 diagram. The first group of crystals are typically erionite-Ca having Ca^{2+} as the dominant EF cation, while K^+ is slightly subordinate and Na^+ is present in low amounts. The second group of crystals display a composition that falls in the central part of the triangular plot, corresponding to comparable amounts of the EF cations Ca^{2+}, K^+, and Na^+. Unfortunately, these two chemical populations of crystals do not correspond to any difference in morphology and/or physical properties, making their distinction not possible utilizing only macro- and/or microscopic investigations. For this reason, in this sample there is reference to an intermediate composition between those of the two populations.

The prismatic to acicular erionite from MF2 has an average chemical formula $(Na_{2.43}K_{2.08}Ca_{1.59}Mg_{0.28})[Al_{8.72}Si_{27.28}O_{72}]\cdot 29.90H_2O$. According to the prevailing EF cation (Na^+: 2.23–2.75 *apfu*), it is classified as erionite-Na. However, because significant amounts of other EF cations are also present (K^+: 1.92–2.32 *apfu*; Ca^{2+}: 1.30–2.18 *apfu*), the composition of this sample falls toward the central part of the classification diagram of erionite (Figure 4). The Mg^{2+} content ranges from 0.04 to 0.52 *apfu* corresponding to a Mg/(Ca +Na) ratio of 0.07 (range 0.01–0.13).

The acicular to fibrous erionite from MB170 is classified as erionite-Ca (Figure 4) according to its average chemical formula $(Ca_{2.77}K_{2.44}Na_{0.46}Mg_{0.33})[Al_{9.09}Si_{26.91}O_{72.01}]\cdot 30.02H_2O$. Ca^{2+} is the prevailing EF cation (2.44–3.09 *apfu*), but K^+ is only slightly less abundant (2.05–2.81 *apfu*). In contrast, Na^+ content is lower (0.28–0.65 *apfu*) and comparable to that of Mg^{2+} (0.22–0.45 *apfu*: Mg/(Ca +Na) = 0.10, range 0.08–0.16).

The extremely fibrous erionite from BV201 displays an average chemical formula $(Ca_{3.51}K_{2.21}Na_{0.39}Mg_{0.26})[Al_{10.35}Si_{25.65}O_{72}]\cdot 30.23H_2O$ and classified as erionite-Ca (Figure 4). Ca^{2+} content ranges from 2.96 to 3.81 *apfu*, whereas that of K^+ is consistently lower (1.93–2.56 *apfu*). Similar to MB170, the Na^+ content (0.14–0.87 *apfu*) is comparable to that of Mg^{2+} (0.03–0.43 *apfu*: Mg/(Ca+Na) = 0.07, range 0.01–0.11).

Structure of the fibrous samples

A full structure refinement was carried out for erionite and levyne (sample BV201) and erionite (sample MB170). However, due to the presence of a mixture of two phases occurring almost exactly at 50 wt % (sample BV201), it is postulated that the structural results are less accurate than those retrieved for sample MB170, in particular, as far as the EF cation and water molecules position and population is referred to. Therefore, in this section mainly the structural features of MB170 are described. Fractional coordinates, isotropic displacement parameters, site multiplicity and occupancy, and site scattering of MB170 are reported in Table 4. Relevant bond distances and contacts are presented in Table 5. Fractional coordinates, isotropic displacement parameters, site multiplicity and occupancy, and site scattering of BV201 are provided in Supplementary Material, Table S2.

The cell parameters and volume of samples BV201 and MB170 are a = 13.34082(19) Å, c = 15.1229(3) Å, V = 2330.94(8) Å^3 and a = 13.31490(13) Å, c = 15.09267(19) Å, V = 2317.25(5) Å^3, respectively (Table 2). Owing to the fact that in recent years several samples of fibrous erionite were characterized in detail from the crystal chemical and structural point of view, a new graph, reporting the dependence of the cell volume on $R = \frac{Si}{Si+Al}$ derived from chemical data (Figure 5), is proposed. This relationship was first reported by Passaglia, Artioli, and Gualtieri (1998) using a set of 23 samples that were implemented in

Table 4.

Site	*x*	y	z Framework	B_{iso}(Å^2)	Site occ.	s.s.(e$^-$)	Proposed site partition	s.s.(e$^-$) from site partition
T1	0.23230(16)	−0.0028(2)	0.10423(9)	0.94(2)	1		$Si_{17.08}Al_{6.92}$	
T2	0.0943(2)	0.4263(2)	1/4	0.94(2)	1		$Si_{10.09}Al_{1.91}$	
O1	0.3505(3)	0.0263(3)	0.6626(3)	1.74(7)	1			
O2	0.09763(20)	2*x*	0.1261(4)	1.74(7)	1			
O3	0.1265(2)	2*x*	0.6310(4)	2.74(11)	1			
O4	0.2719(3)	0	0	1.74(7)	1			
O5	0.2318(3)	2*x*	1/4	2.74(11)	1			
O6	0.4531(3)	2*x*	1/4	2.74(11)	1			
			EF cations					
Ca1	1/3	2/3	0.9368(13)	12.43(19)	0.71(2)	57.0(20)	$Mg_{0.33}Ca_{2.27}$	49.4
Ca2	1/3	2/3	0.1066(12)	12.43(19)	0.312(6)	24.9(5)	$Na_{0.46}$	5.1
Ca3	1/3	2/3	0.626(8)	12.43(19)	0.13(2)	10.1(19)	$Ca_{0.50}$	10.0
K1	0	0	1/4	1.57(11)	1	38	$K_{2.00}$	38.0
K2	1/2	0	0	1.57(11)	0.065(10)	7.4(11)	$K_{0.41}$	7.8
					$\Sigma_{cat.}$	137(5)		110.2
			Water molecules					
OW7	0.245(4)	2*x*	3/4	6.22(9)	0.23(5)	11(2)		
OW8	0.2510(4)	2*x*	0.0160(9)	12.43(19)	0.802(6)	77.0(6)		
OW9	0.4317(6)	2*x*	0.8943(10)	12.43(19)	0.781(11)	75.0(10)		
OW10	0.4126(17)	2*x*	0.705(3)	12.43(19)	0.57(3)	55(3)		
OW11	0.2446(13)	2*x*	0.692(2)	12.43(19)	0.219(13)	21.0(12)		
OW12	0.4707(11)	2*x*	0.0330(18)	12.43(19)	0.463(15)	44.4(14)		
					Σ_{water}	284(9)		

Table 5.

T1	-O2	1.629(2)	T2	-O6	1.609(4)
	-O3	1.652(4)		-O1 x2	1.632(4)
	-O4	1.654(2)		-O5	1.640(4)
	-O1	1.660(5)			
			K2	-OW12	*0.84(2)*
K1	-O2 x6	2.972(5)		-OW9 x2	*2.243(14)*
	-O3 x6	3.427(5)		-O4 x2	3.037(4)
				-O1 x4	3.287(5)
Ca1	-OW8 x3	2.244(15)		-OW8 x4	3.338(12)
	-OW9 x3	2.356(15)			
	-OW10 x3	2.82(5)	Ca2	-OW8 x3	2.341(15)
	-OW11 x3	2.83(3)		-O5 x3	3.188(13)
				-OW12	*3.36(2)*
Ca3	-OW10 x3	2.19(8)	Ca1	-Ca3	*0.94(13)*
	-OW11 x3	2.28(6)	OW7	-OW11	*0.87(4)*
	-OW9 x3	2.29(2)		-OW10	*2.05(5)*
	-OW7 x3	2.76(11)	OW9	-OW10	*1.56(5)*
	-OW8 x3	2.86(10)		-OW12	*2.28(3)*
	-OW10 x3	3.14(11)	OW10	-OW10	*1.36(10)*
				-OW11	*1.96(2)*
			OW11	-OW11	*1.74(7)*

the present investigation with nine further samples. The new equation $R = \frac{Si}{Si+Al} = -0.021 + 5.593$ has a correlation factor R (unfortunately it takes the same symbol of the Si fraction) of 0.98 (R^2 = 0.96), which represents an improvement with respect to the value of 0.96 reported by Passaglia, Artioli, and Gualtieri (1998). It is worth noting that erionite-K is consistently characterized by a smaller volume (and a higher$R = \frac{Si}{Si+Al}$) than that of erionite-Ca. In contrast, a few fibrous samples of erionite-Na are characterized by a volume comparable to that of erionite-K.

The cell parameters of levyne-Ca associated with erionite in sample BV201 are a = 13.32924 (12) Å, c = 22.9296(3) Å, V = 3528.08(8) Å^3. Owing to the small dimensions of the crystals and the "sandwich-like" morphology, it was not possible to retrieve a reliable chemical composition. Microstructural parameters were obtained by the analysis of the integral breadths β_i of the individual reflections (Ballirano and Sadun 2009). In particular, in the case of BV201 a volume-weighted mean column height L_{vol} of 72.3(9) nm and ε_0 micro-strain (lattice strain) of 0.0736(17) were obtained. In the case of MB170, an attempt to apply an ellipsoid modeling of the average shape of the crystallites using the approach of Katerinopoulou, Balic-Zunic, and Lundegaard (2012) was undertaken. In the hexagonal system, the shape ellipsoid parameters b_{ij} are constrained as $b_{11} = b_{22} = 2b_{12}$; $b_{13} = b_{23} = 0$. The orientation of the ellipsoid is such that the principal radii r_a ⊠ c and r_c ⊠ c. Nevertheless, the refined r_a and r_c radii were of 576(9) and 567(11) nm indicating an isotropic coherency domain that is of one order of magnitude greater than that of BV201. This is in agreement with the results of the morphological analysis by ESEM (see above). Micro-strain was significantly smaller than that of BV201 as indicated by ε_0 value of 0.0445(17). The moderate strain of BV201 is related to curling of the fibrils (Cametti et al. 2013) and possibly to the requirement to maintain some coherency at the boundary with levyne that has a slightly smaller a-parameter as compared to erionite.

The mean bond distances <T1-O ≥ 1.649 Å and <T2-O ≥ 1.629 Å of MB170 are consistent with a disordered Si/Al distribution (<T1-O>—<T2-

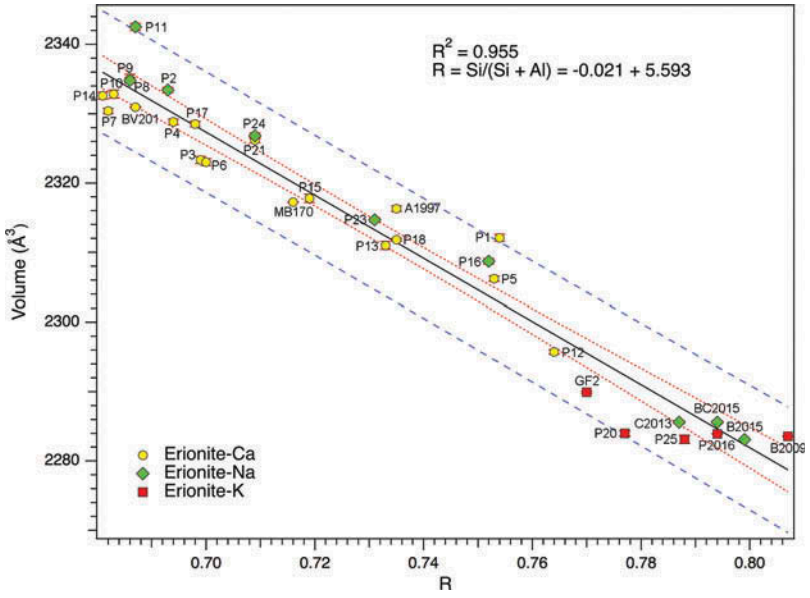

Figure 5.

O ≥ 0.020 Å) leading to a preferential partition of Al at the tetrahedral T1 site (Table 6). This behavior represents a novelty as our previous structure refinements of fibrous erionite-K and erionite-Na samples (Ballirano et al. 2009; Ballirano and Pacella 2016, 2015; Cametti et al. 2013; Pacella, Ballirano, and Cametti 2016) consistently indicated a preferential partition of Al at tetrahedral T2 site, whereas the sample of prismatic erionite-Ca from Nizhnyaya Tunguska, Siberia, analyzed by Alberti et al. (1997) was characterized by an almost identical distribution between T1 and T2. Two R ratios were calculated by using both the Jones' determinative curves (Jones 1968) based upon <T-O> (R_{Jones}) and the regression equation based upon cell volume, modified from Passaglia, Artioli, and Gualtieri (1998), and derived in the present investigation (R_{Vol}). An R_{Jones} value of 0.755, resulting from the population of the T1 ($Al_{6.92}Si_{17.08}$) and T2 ($Al_{1.91}Si_{10.09}$) sites, was determined, as well as an R_{Vol} value of 0.727 (Table 6). Those values are reasonably close with that of 0.748 obtained from chemical data (R_{Che}). Similarly, the R_{Jones} and R_{Vol} values of 0.714 and 0.698, respectively, were obtained for erionite BV201, both comparing favorably with R_{Che} of 0.713 (Table 6). Simultaneously, an R_{Jones} value of 0.729 was calculated for levyne occurring in association with erionite in sample BV201. This value exceeds that commonly observed in levyne samples (0.62 < R < 0.70; Passaglia and Sheppard 2001). However, as indicated by Ballirano and Cametti (2013) a relatively high underestimation of the Al content from <T-O> was found as compared to chemical data for levyne samples.

SEM-EDS analysis of MB170 indicates a total site scattering (*s.s.*) of the EF cations of 110(10) e^-. This value is in agreement with the *s.s.* of 137 (5) e^- obtained from the Rietveld refinement (Table 4). The relatively low *s.s.* resulting from SEM-EDS may be reasonably attributed to EF cations mobilization. Further, a total of 35.5 (11) water molecules *pfu* were allocated by the refinement, in agreement with reference data (Coombs et al. 1997; Passaglia, Artioli, and Gualtieri 1998), albeit numerically higher. The structure is similar to that of erionite-Ca from Nizhnyaya Tunguska, Siberia (Alberti et al. 1997), except for minor differences in EF cation and water molecule sites population. Electron density was detected at the K2 site and, consistently with the chemical analysis, attributed to K cations in excess of 2 *apfu*. It was found that the refined *s.s.* of K1 + K2 agrees with the K content quantified by SEM-EDS. Therefore, one might expect that the relatively large difference between the total EF *s.s.* retrieved from the Rietveld refinement and that from the chemical

Table 6.

Sample	Species	<T1-O>	<T2-O>	T1	T2	T	R_{Jones}	R_{Vol}	R_{Chem}
BV201	Erionite (46.08(16) wt.%)	1.6477	1.6492	$Al_{6.78}Si_{17.22}$	$Al_{3.50}Si_{8.50}$	$Al_{10.28}Si_{25.72}$	0.714	0.698	0.713
	Levyne (53.92(16) wt.%)	1.6437	1.6503	$Al_{9.24}Si_{26.76}$	$Al_{5.38}Si_{12.62}$	$Al_{14.62}Si_{39.38}$	0.729	-	-
MB170	Erionite	1.6486	1.6285	$Al_{6.92}Si_{17.08}$	$Al_{1.91}Si_{10.09}$	$Al_{8.83}Si_{27.17}$	0.755	0.727	0.748

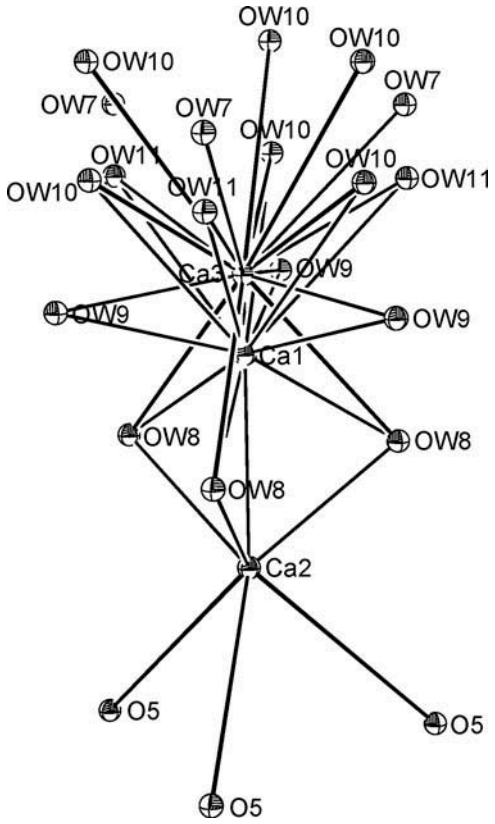

Figure 6.

data may be predominantly assigned to Na volatilization occurring during the micro-chemical analysis. EF cation sites coordination is illustrated in Figure 6. A reasonable sixfold coordination for Ca may be observed at Ca1 considering 3 x OW8 at 2.244(15) Å and 3 x OW10 at 2.82(5) Å. Similarly, to the sample of erionite-Ca investigated by Alberti et al. (1997), an anomalous coordination of Ca2 was found. In fact, the present refinement indicates a ninefold coordination to 3 x OW8 at 2.341(15) Å, 3 x O5 at 3.188(13) Å, and 3 x OW12 at a long 3.36(2) Å distance, which is potentially compatible with the occurrence of Na. However, the refined *s.s.* of 24.9(5) e^- largely exceeds that potentially provided by all available Na (ca. 5 e^-). Two hypotheses may be proposed to justify this result, a significant volatilization of Na during SEM-EDS analysis and/or the occurrence of static disorder impossible to model under the present experimental conditions. A reasonable sixfold coordination for Ca may be noted at Ca3 considering 3 x OW9 at 2.29(2) Å and 3 x OW7 at 2.76(11) Å.

Erionite occurrences and risk assessment in Italy

The initial findings of erionite in Italy date back to the 1970s, when Passaglia and Galli (1974) and Pongiluppi, Passaglia, and Galli (1974) reported the presence of erionite within basic volcanic rocks in Montresta (OR) and Nurri (CA) areas, Sardinia region. Data indicated that the erionite crystals occur as a sub-millimeter coating of slight thin fibers in epitaxial growth with levyne crystals, forming a typical sandwich-like intergrowth. Those crystals were found in vugs and cavities of weathered andesites and basalts. In the same period, Giovagnoli and Boscardin (1979) detected the presence of erionite as fibrous spherulitic aggregates within amygdaloidal basalts at Montecchio Maggiore (VI), Veneto region. Successively, erionite was also found in the Tertiary volcanites (latitic and trachytic lavas) in the Euganean Hills, Veneto region (Passaglia and Tagliavini 1995). In this case, erionite occurs as clear-white radiating bundles of needles 2–3 mm long, with a chemical composition dominated by Ca as EF cation. Examination of secondary mineral assemblages in the Tertiary volcanic rocks of the Lessini Mountains indicated a significant occurrence of erionite (Cenni 2009; Mattioli, Cenni, and Passaglia 2016a), which is present in 65% of the investigated outcrops, with an estimated amount varying from 10 to 40 vol% of the total secondary minerals. In these volcanic rocks, erionite also displayed different morphological types, ranging from prismatic crystals with "rigid" behavior to extremely fibrous with flexible "hair-like" appearance (Giordani et al. 2016). These features, combined with the significant amounts reported above, raise concern for adverse effects on human health, especially if one considers that these basalts often host active mining or quarrying activities and that these rocks are extensively used as aggregate in asphalt and concrete pavements, as a road base, railroad ballast and cobblestone pavement. Nonetheless, a detailed description and quantification of erionite present in all of these areas are still lacking.

In addition to these erionite occurrences, it is of importance to consider that there are many other volcanic rocks, such as ignimbrites, lavas, and tuffaceous sediments, which extensively crop out in

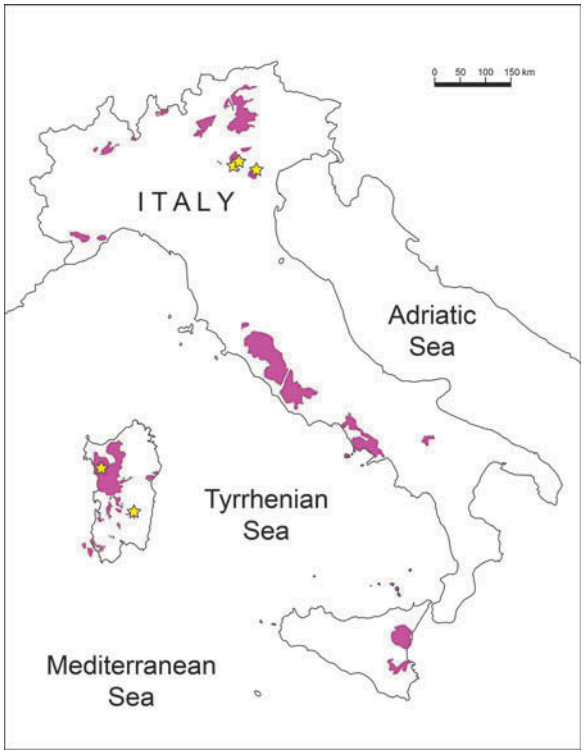

Figure 7.

further regions of Italy, especially Lazio and Campania (Figure 7). It is relevant to note that most of these volcanites possess a huge thickness and are affected by a variety of secondary mineralization processes similar to those described in other areas where erionite has been widely found (Ortega-Guerrero and Carrasco-Nùñez 2014; Saini-Eidukat and Triplet 2014; Van Gosen et al. 2013). Therefore, it cannot be excluded *a priori* that erionite, or some other fibrous zeolites, might also be extensively present in these volcanic rocks. Nevertheless, most of these rocks have not apparently been investigated with this aim in mind and specific studies on the occurrence of fibrous minerals are currently lacking. Given the huge extension of these volcanic rocks, the possibility of an environmental exposure to this hazardous fibrous zeolite needs to be taken into serious consideration.

The discovery of fibrous erionite in the Lessini Mountains, coupled with its occurrence as fibers of inhalable size (Giordani et al. 2016), suggests the need for a detailed risk assessment in Italy. A risk assessment requires coordinated actions from government agencies, local health authorities,

universities, and research centers, in order to record the presence of erionite or other fibrous zeolites, recognizing mineral species and quantifying their abundance in rock deposits. At sites where the presence of fibrous zeolites has been confirmed by lab results, accurate field surveys and sampling campaigns need to be planned, in order to determine detailed geological, stratigraphic, and structural features, measuring the thickness, extent of area affected, and volume of lithostratigraphic units containing these minerals (Vignaroli et al. 2014). These data may be entered into a GIS to produce a result that might be used immediately and in the long period by research institutes, local authorities, and regional agencies for environmental protection. At sites where the presence of hazardous fibrous minerals was confirmed, several airborne fibers sampling campaigns need to be conducted, with the aim to assess the extent of airborne dispersion produced by natural agents and human activity. This is of importance under the situation that these sites host active mining or quarrying activities, where a quantification of the airborne fibers contamination at workplaces is the first fundamental step to propose measures for environmental risk mitigation. In addition to the environmental risk related to the presence of natural erionite, this dangerous fibrous zeolite may also be present in association with other zeolites widely used for various purposes such as petrochemical and nuclear industry, agriculture, medical, and domestic uses.

Further, the knowledge of the epidemiology of mesothelioma linked to erionite in Italy is extremely scarce, and the phenomenon is still little investigated. While mesothelioma cases attributed to asbestos exposure are well known and recorded (INAIL 2012), virtually little is known regarding domestic cases from exposure to airborne erionite fibers. In Italy, it is known that approximately 20% of mesothelioma cases are not linked to asbestos (INAIL 2012). In particular, one of the highest % mesothelioma occurrences in Italy during the time interval 1993–2008 was detected in the Veneto Region. The contribution of exposure to erionite cannot be excluded in this significant %. Unfortunately, epidemiological and public health data that are available according to administrative borders (e.g., provincial or regional areas) do not correspond to the real limits of geological deposits, in this case erionite-containing rocks. Consequently, it is problematic to extrapolate data regarding incidence of mesotheliomas unrelated to asbestos in the Lessini Mountains area which would provide useful information for understanding the contribution of erionite. For this reason, targeted epidemiological surveillance is necessary for a more comprehensive risk assessment and because these findings may be crucial to understand the effect of the choices made in the field of risk management.

Concluding remarks

In this study, new mineralogical, structural, and chemical data of four representative erionite samples (MC35, MF2, MB170, BV201) from Northern Italy were reported, where this carcinogenic zeolite occurs as fibers of inhalable size. The following conclusions may be inferred from the present contribution:

- MC35 is an erionite-Ca characterized by prismatic habit with solid appearance and rigid behavior, and no apparent fibrous elements were detected. MF2 is an erionite-Na formed by acicular crystals with a great tendency to separate fibers and fibrils with rigid behavior. MB170 is an erionite-Ca showing acicular to fibrous crystals, often separating in a great number of small fibrils with rigid to flexible behavior. BV201 is an erionite-Ca with an extremely fibrous, hair-like habit, with flexible appearance and a marked tendency to split up into thin fibers and fibrils. From the structural point of view, MB170 is characterized by an unusual preferred partition of Al at the T1 site instead of T2 as observed in all refinements of erionite samples. A discrepancy between the total EF *s.s.* determined from SEM-EDS and Rietveld refinement was noted that has been attributed to EF cation volatilization/migration (mainly Na) during micro-chemical analysis. A mismatch was detected between the *a*-parameter of erionite-Ca and levyne-Ca that are intergrown in sample BV201. As the single layer of six-membered rings of $(Si,Al)O_4$ tetrahedra, whose stacking along the *z*-axis build both

structures, is common, the mismatch produced some strain that possibly favors the curling of fibrils.

- As a whole, erionite is present in 65% of the investigated outcrops, with an estimated amount varying from 10 to 40 vol% of the total secondary minerals, which are crystallized within vugs and cavities of basaltic rocks. These amounts are significant for effects on human health, especially if one considers that these basalts often host active mining or quarrying activities and that these rocks are extensively used as construction material.
- The discovery of fibrous erionite in the Lessini Mountains suggests the need for a detailed risk assessment in Italy, with specific studies such as a quantification of the potentially airborne fibers and targeted epidemiological surveillance. This need is even more evident if one considers that erionite, or some other fibrous zeolites, might be potentially present in many other volcanic rocks, which extensively crop out in many regions of Italy. Given the large extension of these volcanic rocks, the possibility of an environmental exposure to hazardous fibrous zeolites needs to be given serious consideration. These results provide the basis for health and safety protection programs and for a better scientific understanding of this carcinogenic fibrous zeolite.

Acknowledgments

Special thanks are due to R. Carampin (CNR, Padova) for technical assistance with the microprobe measurements. We are sincerely grateful to the editor-in-chief, Prof. Sam Kacew, for his detailed review of this article and for editorial handling. We also acknowledge the anonymous referees for their very helpful comments and suggestions, which greatly improved the article.

Funding

Funding by Sapienza Università di Roma (P.R. Ateneo 2014 Prof. Ballirano) and Università di Urbino Carlo Bo (FRS DiSPeA 2015 Prof. Mattioli) is warmly acknowledged.

ORCID

Michele Mattioli http://orcid.org/0000-0002-1672-130X

References

Alberti, A., A. Martucci, E. Galli, and G. Vezzalini. 1997. A re-examination of the crystal structure of erionite. *Zeolites* 19:349–52. doi:10.1016/S0144-2449(97)00102-4. Q2

Andujar, P., A. Lacourt, P. Brochard, J.-C. Pairon, M.-C. Jaurand, and D. Jean. 2016. Five years update on relationships between malignant pleural mesothelioma and exposure to asbestos and other elongated mineral particles. *Journal of Toxicology and Environmental Health, Part B* 19:151–72. doi:10.1080/10937404.2016.1193361.

Artvinli, M., and Y. I. Baris. 1979. Malignant mesothelioma in a small village in the Anatolian region of Turkey: An epidemiologic study. *Journal Natural Cancer Institute* 63:17–22.

Aust, A. E., P. M. Cook, and R. D. Dodson. 2011. Morphological and chemical mechanisms of elongated mineral particle toxicities. *Journal of Toxicology and Environmental Health, Part B* 14:40–75. doi:10.1080/10937404.2011.556046.

Ballirano, P. 2003. Effects of the choice of different ionisation level for scattering curves and correction for small preferred orientation in Rietveld refinement: The $MgAl_2O_4$ test case. *Journal of Applied Crystallography* 36:1056–61. doi:10.1107/S0021889803010410.

Ballirano, P. 2011. Laboratory parallel beam transmission X-ray powder diffraction investigation of the thermal behaviour of calcite: Comparison with X-ray single-crystal and synchrotron powder diffraction data. *Period Mineral* 80:123–34.

Ballirano, P., G. B. Andreozzi, M. Dogan, and A. U. Dogan. 2009. Crystal structure and iron topochemistry of erionite-K from Rome, Oregon, U.S.A. *American Mineralogist* 94:1262–70. doi:10.2138/am.2009.3163.

Ballirano, P., and G. Cametti. 2012. Dehydration dynamics and thermal stability of erionite-K: Experimental evidence of the "internal ionic exchange" mechanism. *Microporous and Mesoporous Materials* 163:160–68. doi:10.1016/j.micromeso.2012.06.059.

Ballirano, P., and G. Cametti. 2013. Crystal chemical and structural investigation of levyne-Na. *Mineralogical Magazine* 77:2887–99. doi:10.1180/minmag.2013.077.7.01.

Ballirano, P., and G. Cametti. 2015. Crystal chemical and structural modifications of erionite fibres leached with simulated lung fluids. *American Mineralogist* 100:1003–12. doi:10.2138/am-2015-4922.

Ballirano, P., and A. Pacella. 2016. Erionite-Na upon heating: Dehydration dynamics and exchangeable cations mobility. *Scientific Reports* 6:22786. doi:10.1038/srep22786.

Ballirano, P., A. Pacella, C. Cremisini, E. Nardi, M. Fantauzzi, D. Atzei, A. Rossi, and G. Cametti. 2015. Fe (II) segregation at a specific crystallographic site of fibrous erionite: A

first step toward the understanding of the mechanisms inducing its carcinogenicity. *Microporous and Mesoporous Materials* 211:49–63. doi:10.1016/j.micromeso.2015.02.046.

Ballirano, P., and C. Sadun. 2009. Thermal behaviour of trehalose dihydrate (T_h) and β-anhydrous trehalose (T_β) by in-situ laboratory parallel-beam X-ray powder diffraction. *Structural Chemistry* 20:815–23. doi:10.1007/s11224-009-9473-5.

Baris, I., M. Artvinli, R. Saracci, L. Simonato, F. Pooley, J. Skidmore, and C. Wagner. 1987. Epidemiological and environmental evidence of the health effects of exposure to erionite fibres: A four-year study in the Cappadocian region of Turkey. *International Journal of Cancer* 39:10–17. doi:10.1002/(ISSN)1097-0215.

Baris, Y. I., M. Artvinli, and A. A. Sahin. 1979. Environmental mesothelioma in Turkey. *Annals of the New York Academy of Sciences* 330:423–32. doi:10.1111/j.1749-6632.1979.tb18744.x.

Baris, Y. I., A. A. Sahin, M. Ozesmi, I. Kerse, E. Ozen, B. Kolacan, M. Altinörs, and A. Göktepeli. 1978. An outbreak of pleural mesothelioma and chronic fibrosing pleurisy in the village of Karain/Urgüp in Anatolia. *Thorax* 33:181–92. doi:10.1136/thx.33.2.181.

Baumann, F., and M. Carbone. 2016. Environmental risk of mesothelioma in the United States: An emerging concern-epidemiological issues. *Journal of Toxicology and Environmental Health, Part B* 19:231–49. doi:10.1080/10937404.2016.1195322.

Beccaluva, L., G. Bianchini, C. Bonadiman, M. Coltorti, L. Milani, L. Salvini, F. Siena, and R. Tassinari. 2007. Intraplate litospheric and sublitospheric components in the Adriatic domain: Nephelinite to tholeiite magma generation in the Paleogene Veneto Volcanic Province, Southern Alps. *Mineral Social America, Special Paper* 418:131–52.

Bertino, P., A. Marconi, L. Palumbo, B. M. Bruni, D. Barbone, S. Germano, A. U. Dogan, G. F. Tassi, C. Porta, L. Mutti, and G. Gaudino. 2007. Erionite and asbestos differently cause transformation of human mesothelial cells. *International Journal of Cancer* 121:12–20. doi:10.1002/(ISSN)1097-0215.

Bish, D. L., and D. W. Ming. 2001. Natural zeolites: Occurrence, properties, applications. In eds. D. L. Bish, and D. W. Ming. *Rev Mineral Geochem* 45.

Bloise, A., D. Barca, A. F. Gualtieri, S. Pollastri, and E. Belluso. 2016. Trace elements in hazardous mineral fibres. *Environmental Pollution* 216:314–23. doi:10.1016/j.envpol.2016.06.007.

Bonadiman, C., M. Coltorti, L. Milani, L. Salvini, F. Siena, and R. Tassinari. 2001. Metasomatism in the lithospheric mantle and its relationships to magmatism in the Veneto Volcanic Province, Italy. *Period Mineral* 70:333–57.

Bonneau, L., M. Malard, and H. Pezerat. 1986. Studies on surface properties of asbestos II. Role of dimensional characteristics and surface properties of mineral fibres in the induction of pleural tumors. *Environmental Research* 41:268–75. doi:10.1016/S0013-9351(86)80188-8.

Boulanger, G., P. Andujar, J. C. Pairon, M. A. Billon-Galland, C. Dion, P. Dumortier, P. Brochard, A. Sobaszek, P. Bartsch, C. Paris, and M. C. Jaurand. 2014. Quantification of short and long asbestos fibres to assess asbestos exposure: A review of fiber size toxicity. *Environ Health* 13:59. doi:10.1186/1476-069X-13-59.

Bruker, AXS. 2009. *Topas V.4.2: General profile and structure analysis software for powder diffraction data*. Karlsruhe, Germany: Bruker AXS.

Cametti, G., A. Pacella, F. Mura, M. Rossi, and P. Ballirano. 2013. New morphological, chemical, and structural data of woolly erionite-Na from Durkee, Oregon, U.S.A. *American Mineralogist* 98:2155–63. doi:10.2138/am.2013.4474.

Campbell, L. S., J. Charnock, A. Dyer, S. Hillier, S. Chenery, F. Stoppa, C. M. B. Henderson, R. Walcott, and M. Rumsey. 2016. Determination of zeolite-group mineral composition by electron probe microanalysis (EPMA). *Mineralogical Magazine* 80/5:781–807.

Carbone, M., Y. I. Baris, P. Bertino, B. Brass, S. Comertpay, A. U. Dogan, G. Gaudino, S. Jube, S. Kanodia, C. R. Petridge, H. I. Pass, Z. S. Rivera, I. Steele, M. Tuncer, S. Way, H. Yang, and A. Miller. 2011. Erionite exposure in North Dakota and Turkish villages with mesothelioma. *Proceedings of the National Academy of Sciences* 108:13618–23. doi:10.1073/pnas.1105887108.

Carbone, M., S. Emri, A. U. Dogan, I. Steele, M. Tuncer, H. I. Pass, and Y. I. Baris. 2007. A mesothelioma epidemic in Cappadocia: Scientific developments and unexpected social outcomes. *Nature Reviews. Cancer* 7:147–54. doi:10.1038/nrc2068.

Carbone, M., and H. Yang. 2012. Molecular pathways: Targeting mechanisms of asbestos and erionite carcinogenesis in mesothelioma. *Clinical Cancer Research* 18:598–604. doi:10.1158/1078-0432.CCR-11-2259.

Cenni, M. 2009. Le mineralizzazioni secondarie nelle rocce basaltiche: Esempi dai Monti Lessini (Italia). PhD thesis, University of Urbino, Italy.

Coffin, D. L., P. M. Cook, and J. P. Creason. 1992. Relative mesothelioma induction in rats by mineral fibres: Comparison with residual pulmonary mineral fiber number and epidemiology. *Inhalation Toxicology* 4:273–300. doi:10.3109/08958379209145671.

Cook, P. M., L. D. Palekar, and D. L. Coffin. 1982. Interpretation of the carcinogenicity of amosite asbestos and ferroactinolite on the basis of retained fiber dose and characteristics in vivo. *Toxicology Letters* 13:151–58. doi:10.1016/0378-4274(82)90203-X.

Coombs, D. S., A. Alberti, T. Armbruster, G. Artioli, C. Colella, E. Galli, J. D. Grice, F. Liebau, J. A. Mandarino, H. Minato, E. H. Nickel, E. Passaglia, D. R. Peacor, S. Quartieri, R. Rinaldi, M. Ross, R. A. Sheppard, E. Tillmanns, and G. Vezzalini. 1997. Recommended nomenclature for zeolite minerals: Report of the subcommittee on zeolites of the International Mineralogical Association, Commission on New Minerals and Mineral Names. *Canadian Mineralogist* 35:1571–606.

Croce, A., M. Musa, M. Allegrina, C. Rinaudo, Y. I. Baris, A. U. Dogan, A. Powers, Z. Rivera, P. Bertino, H. Yang, G.

Gaudino, and M. Carbone. 2013. Micro-Raman spectroscopy identifies crocidolite and erionite fibers in tissue section. *Journal of Raman Spectroscopy* 44:1440–45. doi:10.1002/jrs.v44.10.

Crovella, S., A. M. Bianco, J. Vuch, L. Zupin, R. R. Moura, E. Trevisan, M. Schneider, A. Brollo, E. M. Nicastro, A. Cosenzi, G. Zabucchi, and V. Borelli. 2016. Iron signature in asbestos-induced malignant pleural mesothelioma: A population-based autopsy study. *Journal of Toxicology and Environmental Health, Part A* 79:129–41. doi:10.1080/15287394.2015.1123452.

Davis, J. M. G., R. E. Bolton, B. G. Miller, and K. Niven. 1991. Mesothelioma dose response following intraperitoneal injection of mineral fibres. *International Journal of Experimental Pathology* 72:263–74.

de Assis, L. V. M., J. Locatelli, and M. C. Isoldi. 2014. The role of key genes and pathways involved in the tumorigenesis of malignant mesothelioma. *Biochimica Et Biophysica Acta* 1845:232–47.

De Vecchi, G. P., and R. Sedea. 1995. The Paleogene basalt of the Veneto region (NE Italy). *Memory Ist Geological Mineral, University Padova* 47:253–74.

Deer, W. A., R. Howie, W. S. Wis, and J. Zussman. 2004. *Rock forming minerals. Framework silicates: Silica minerals, feldspathoids and the zeolites*. London, UK: 4B, The Geological Society.

Demirer, E., C. F. Ghattas, M. O. Radwan, and E. M. Elamin. 2015. Clinical and prognostic features of erionite-induced malignant mesothelioma. *Yonsei Medical Journal* 56:311–23. doi:10.3349/ymj.2015.56.2.311.

Dodson, R. F., M. A. L. Atkinson, and J. L. Levin. 2003. Asbestos fiber length as related to potential pathogenicity: A critical review. *American Journal of Industrial Medicine* 44:291–97. doi:10.1002/ajim.10263.

Dogan, A. U. 2003. Zeolite mineralogy and Cappadocian erionite. *Indoor and Built Environment* 12:337–42. doi:10.1177/142032603036408.

Dogan, A. U., Y. I. Baris, M. Dogan, S. Emri, I. Steele, A. G. Elmishad, and M. Carbone. 2006. Genetic predisposition to fiber carcinogenesis causes a mesothelioma epidemic in Turkey. *Cancer Research* 66:5063–68. doi:10.1158/0008-5472.CAN-05-4642.

Dogan, A. U., and M. Dogan. 2008. Re-evaluation and reclassification of erionite series minerals. *Environ Geochem Health* 30:355–66. doi:10.1007/s10653-008-9163-z.

Dogan, A. U., M. Dogan, and J. A. Hoskins. 2008. Erionite series minerals: Mineralogical and carcinogenic properties. *Environ Geochem Health* 30:367–81. doi:10.1007/s10653-008-9165-x.

Dogan, M. 2012. Quantitative characterization of the mesothelioma-inducing erionite series minerals by transmission electron microscopy and energy dispersive spectroscopy. *Scanning* 34:37–42. doi:10.1002/sca.20276.

Eakle, A. S. 1898. Erionite, a new zeolite. *American Journal of Science* 6:66–68. doi:10.2475/ajs.s4-6.31.66.

Emri, S., A. Demir, M. Dogan, H. Akay, B. Bozkurt, M. Carbone, and I. Baris. 2002. Lung diseases due to environmental exposures to erionite and asbestos in Turkey. *Toxicology Letters* 127:251–57. doi:10.1016/S0378-4274(01)00507-0.

Farrugia, L. J. 1999. *ORTEP-3 for Windows*. Scotland: University of Glasgow.

Fubini, B. 2001. The physical and chemical properties of asbestos fibres which contribute to biological activity. Asbestos Health Effect Conference, May 24-25, Oakland, CA, US Environmental Protection Agency.

Gazzano, E., C. Riganti, M. Tomatis, F. Turci, A. Bosia, B. Fubini, and D. Ghigo. 2005. Potential toxicity of nonregulated asbestiform minerals: Balangeroite from the Western Alps. Part 3: Depletion of antioxidant defenses. *Journal of Toxicology and Environmental Health, Part A* 68:41–49. doi:10.1080/15287390590523957.

Giordani, M., M. Mattioli, M. Dogan, and A. U. Dogan. 2016. Potential carcinogenic erionite from Lessini Mounts, NE Italy: Morphological, mineralogical and chemical characterization. *Journal of Toxicology and Environmental Health, Part A* 79:808–24. doi:10.1080/15287394.2016.1182453.

Giovagnoli, L., and M. Boscardin. 1979. Ritrovamento di levyna ed erionite a Montecchio Maggiore (Vicenza). *Riv Mineral Ital* 1:44–45.

Goldstein, J. I., D. E. Newbury, P. Echlin, D. C. Joy, A. D. Roming, C. E. Lyman, C. Fiori, and E. Lifshin. 1992. *Scanning electron microscopy and X-ray microanalysis*, 2nd ed. New York, USA: Plenum Press.

Gottardi, G., and E. Galli. 1985. *Natural zeolites*. Heidelberg, Germany: Springer-Verlag.

Gualtieri, A., G. Artioli, E. Passaglia, S. Bigi, A. Viani, and J. C. Hanson. 1998. Crystal structure-crystal chemistry relationships in the zeolites erionite and offretite. *American Mineralogist* 83:590–606. doi:10.2138/am-1998-5-619.

Gude, A. J., and R. A. Sheppard. 1981. Woolly erionite from the Reese River zeolite deposit, Lander County, Nevada, and its relationship to other erionites. *Clays Clay Minerals* 29:378–84. doi:10.1346/CCMN.1981.0290507.

Hesterberg, T. W., G. Chase, C. Axten, W. C. Miller, R. P. Musselman, O. Kamstrup, J. Hadley, C. Morscheidt, D. M. Bernstein, and P. Thevenaz. 1998. Biopersistence of synthetic vitreous fibers and amosite asbestos in the rat lung following inhalation. *Toxicology and Applied Pharmacology* 151:262–75. doi:10.1006/taap.1998.8472.

Hill, R. J., R. E. Edwards, and P. Carthew. 1990. Early changes in the pleural mesothelium following intrapleural inoculation of the mineral fibre erionite and the subsequent development of mesotheliomas. *British Journal of Experimental Pathology* 71:105–18.

Hillegass, J. M., J. M. Miller, M. B. MacPherson, C. M. Westbom, M. Sayan, J. K. Thompson, S. L. Macura, T. N. Perkins, S. L. Beuschel, V. Alexeeva, H. I. Pass, C. Steele, B. T. Mossman, and A. Shukla. 2013. Asbestos and erionite prime and activate the NLRP3 inflammasome that stimulates autocrine cytokine release in human mesothelial cells. *Particle and Fibre Toxicology* 10:39. doi:10.1186/1743-8977-10-39.

Hochella, M. F. 1993. Surface chemistry, structure, and reactivity of hazardous mineral dust. In Health effects of mineral dusts, eds. G. D. Guthrie and B. T. Mossman. Chelsea, MI: Bookcrafters. *Reviews Mineral* 28:275–308.

IARC. 1987. Overall evaluations of carcinogenicity: An updating of IARC monographs volumes 1 to 42. In *IARC monographs on the evaluation of carcinogenic risks to human*, vol. 7. Lyon.

IARC. 1997. Zeolites other than erionite. In *Silica, some silicates, coal dust and para-aramid fibrils. IARC monographs on the evaluation of carcinogenic risks to human*, vol. 68. Lyon.

IARC. 2012. Arsenic, metals, fibres, and dusts. In *IARC monographs on the evaluation of carcinogenic risks to human*, vol. 100C. Lyon.

Ilgren, E. B., H. Kazemian, and J. A. Hoskins. 2015. Kandovan the next Capadoccia? A potential public health issue for erionite related mesothelioma risk. *Epidemiol, Biostatistics Public Health* 12:1–12.

INAIL. 2012. *Il Registro Nazionale dei Mesoteliomi (ReNaM): Quarto rapporto*. Roma: INAIL, Settore Ricerca, Dipartimento Medicina del Lavoro.

Jacobsen, S. D., J. R. Smyth, R. F. Swope, and R. T. Downs. 1998. Rigid body character of the SO_4 group in celestine, anglesite and barite. *Canadian Mineralogist* 36:1053–60.

Jones, J. B. 1968. Al-O and Si-O tetrahedral distances in aluminosilicate framework structures. *Acta Crystallographica Section B Structural Crystallography and Crystal Chemistry* 24:355–58. doi:10.1107/S0567740868002360.

Katerinopoulou, A., T. Balic-Zunic, and L. F. Lundegaard. 2012. Application of the ellipsoid modeling of the average shape of nanosized crystallites in powder diffraction. *Journal of Applied Crystallography* 45:22–27. doi:10.1107/S0021889811055075.

Kliment, C. R., K. Clemens, and T. D. Oury. 2009. North American erionite-associated mesothelioma with pleural plaques and pulmonary fibrosis: A case report. *International Journal of Clinical and Experimental Pathology* 2:407–10.

Kokturk, N., P. Firat, H. Akay, C. Kadilar, C. Ozturk, F. Zorlu, Y. Gungen, and S. Emri. 2005. Prognostic significance of Bax and Fas Ligand in erionite and asbestos induced Turkish malignant pleural mesothelioma. *Lung Cancer* 50:189–98. doi:10.1016/j.lungcan.2005.05.025.

Larson, D., A. Powers, J.-P. Ambrosi, M. Tanjia, A. Napolitano, E. G. Flores, F. Baumann, L. Pellegrini, C. J. Jennings, B. J. Buck, B. T. McLaurin, D. Merkler, C. Robinson, P. Morris, M. Dogan, A. U. Dogan, H. I. Pass, S. Pastorino, M. Carbone, and H. Yanga. 2016. Investigating palygorskite's role in the development of mesothelioma in southern Nevada: Insights into fiber-induced carcinogenicity. *Journal of Toxicology and Environmental Health, Part B* 19:213–30. doi:10.1080/10937404.2016.1195321.

Lee, K. P. 1985. Lung response to particulates with emphasis on asbestos and other fibrous dusts. *Crc Critical Reviews in Toxicology* 14:33–86. doi:10.3109/10408448509023764.

Lemen, R. A. 2016. Mesothelioma from asbestos exposures: Epidemiologic patterns and impact in the United States. *Journal of Toxicology and Environmental Health, Part B* 19:250–65. doi:10.1080/10937404.2016.1195323.

Lippmann, M. 1988. Asbestos exposure indices. *Environmental Research* 46:86–106. doi:10.1016/S0013-9351(88)80061-6.

Mattioli, M., M. Cenni, and E. Passaglia. 2016a. Secondary mineral assemblages as indicators of multistage alteration processes in basaltic lava flows: Evidence from the Lessini Mountains, Veneto Volcanic Province, Northern Italy. *Period Mineral* 85:1–24.

Mattioli, M., M. Giordani, M. Dogan, M. Cangiotti, G. Avella, R. Giorgi, A. U. Dogan, and M. F. Ottaviani. 2016b. Morpho-chemical characterization and surface properties of carcinogenic zeolite fibres. *Journal of Hazardous Materials* 306:140–48. doi:10.1016/j.jhazmat.2015.11.015.

Mattioli, M., M. Lustrino, S. Ronca, and G. Bianchini. 2012. Alpine subduction imprint in Apennine volcaniclastic rocks. Geochemical–petrographic constraints and geodynamic implications from Early Oligocene Aveto-Petrignacola Formation (N Italy). *Lithos* 134:201–20. doi:10.1016/j.lithos.2011.12.017.

Maxim, D. L., J. G. Hadley, R. M. Potter, and R. Niebo. 2006. The role of fiber durability/biopersistence of silica-based synthetic vitreous fibres and their influence on toxicology. *Regulatory Toxicology and Pharmacology* 46:42–62. doi:10.1016/j.yrtph.2006.05.003.

Metintas, M., G. Hillerdal, and S. Metintas. 1999. Malignant mesothelioma due to environmental exposure to erionite: Follow-up of a Turkish emigrant cohort. *European Respiratory Journal* 13:523–26. doi:10.1183/09031936.99.13352399.

Metintas, M., G. Hillerdal, S. Metintas, and P. Dumortier. 2010. Endemic malignant mesothelioma: Exposure to erionite is more important than genetic factors. *Archives of Environmental & Occupational Health* 65:86–93. doi:10.1080/19338240903390305.

Milani, L., L. Beccaluva, and M. Coltorti. 1999. Petrogenesis and evolution of the Euganean magmatic complex, Veneto Region, North-East Italy. *European Journal Mineral* 11:379–99. doi:10.1127/ejm/11/2/0379.

Millette, J. R. 2006. Asbestos analysis methods. In *Asbestos-Risk Assessment, Epidemiology, and Health Effects*, eds. R. F. Dodson, and S. P. Hammar, 9–37. Boca Raton, FL: Taylor and Francis.

Muhle, H., B. Bellmann, and F. Pott. 1991. Durability of various mineral fibres in rat lungs, mechanisms in fibre carcinogenesis. In *NATO ASI series A: Life Sciences*, eds. R. C. Brown, J. A. Hoskins, and N. F. Johnson, vol. 223, 181–87. New York: Plenum Press.

Oberdorster, G., V. Castranova, B. Asgharian, and P. Sayre. 2015. Inhalation exposure to carbon nanotubes (CNT) and carbon nanofibers (CNF): Methodology and dosimetry. *Journal of Toxicology and Environmental Health, Part B* 18:121–212. doi:10.1080/10937404.2015.1051611.

Oberdörster, G., E. Oberdörster, and J. Oberdörster. 2005. Nanotoxicology: An emerging discipline evolving from studies of ultrafine particles. *Environmental Health Perspectives* 113:823–39. doi:10.1289/ehp.7339.

Ortega-Guerrero, M. A., and G. Carrasco-Nùñez. 2014. Environmental occurrence, origin, physical and geochemical properties, and carcinogenic potential of erionite near San Miguel de Allande, Mexico. *Environ Geochem Health* 36:517–29. doi:10.1007/s10653-013-9578-z.

Ortega-Guerrero, M. A., G. Carrasco-Núñez, H. Barragán-Campos, and M. R. Ortega. 2015. High incidence of lung cancer and malignant mesothelioma linked to erionite fibre exposure in a rural community in Central Mexico. *Occupational and Environmental Medicine* 72:216–18. doi:10.1136/oemed-2013-101957.

Pacella, A., P. Ballirano, and G. Cametti. 2016. Quantitative chemical analysis of erionite fibres using a micro-analytical SEM-EDX method. *European Journal of Mineralogy* 28:257–64. doi:10.1127/ejm/2015/0027-2497.

Passaglia, E. 1970. The crystal chemistry of chabazites. *American Mineral* 55:1278–301.

Passaglia, E., G. Artioli, and A. Gualtieri. 1998. Crystal chemistry of the zeolites erionite and offretite. *American Mineralogist* 83:577–89. doi:10.2138/am-1998-5-618.

Passaglia, E., and E. Galli. 1974. Levyne and erionite from Sardinia, Italy. *Contributions to Mineralogy and Petrology* 43:253–59. doi:10.1007/BF00373482.

Passaglia, E., and A. R. Sheppard. 2001. The crystal chemistry of zeolites. In natural zeolites: Occurrence, properties, applications (D.L. Bish and D.W. Ming, editors) Mineralogical Society of America and the Geochemical Society, Washington, D.C. *Reviews in Mineralogy and Geochemistry* 45:69–116. doi:10.2138/rmg.2001.45.2.

Passaglia, E., and A. Tagliavini. 1995. Erionite from Faedo, Colli Euganei, Italy. *Neues Jahrbuch Mineralogie-Monatshefte* 185–91.

Pollastri, S., F. D'Acapito, A. Trapananti, I. Colantoni, G. B. Andreozzi, and A. F. Gualtieri. 2015. The chemical environment of iron in mineral fibres. A combined X-ray absorption and Mössbauer spectroscopic study. *Journal of Hazardous Materials* 298:282–93. doi:10.1016/j.jhazmat.2015.05.010.

Pollastri, S., A. F. Gualtieri, M. L. Gualtieri, M. Hanuskova, A. Cavallo, and G. Gaudino. 2014. The Zeta potential of mineral fibres. *Journal of Hazardous Materials* 276:469–79. doi:10.1016/j.jhazmat.2014.05.060.

Pongiluppi, D., E. Passaglia, and E. Galli. 1974. Su alcune zeoliti della Sardegna. *Social Ital Mineral Petrol* 30:77–100.

Pott, F., U. Ziem, F. J. Reiffer, F. Huth, H. Ernst, and U. Mohr. 1987. Carcinogenicity studies on fibres, metal compounds, and some other dusts in rats. *Experimental Pathology* 32:129–52. doi:10.1016/S0232-1513(87)80044-0.

Reed, S. J. B. 1993. *Electron microprobe analysis*, 2nd ed. Cambridge, UK: Cambridge University Press.

Rinaldi, R. 1976. Crystal chemistry and structural epitaxy of offretite-erionite from Sasbach, Kaiserstuhl. *Neues Jahrbuch Mineralogie-Monatshefte* 145–56.

Sabine, T. M., B. A. Hunter, W. R. Sabine, and C. J. Ball. 1998. Analytical expressions for the transmission factor and peak shift in absorbing cylindrical specimens. *Journal of Applied Crystallography* 31:47–51. doi:10.1107/S0021889897006961.

Sacerdoti, M. 1996. New refinements of the crystal structure of levyne using twinned crystals. *Neues Jahrbuch Mineralogie-Monatshefte* 114–24.

Saini-Eidukat, B., and J. W. Triplet. 2014. Erionite and offretite from the Killdeer Mountains, Dunn County, North Dakota, USA. *American Mineralogist* 99:8–15. doi:10.2138/am.2014.4567.

Sheppard, R. A., and A. J. Gude. 1969. Chemical composition and physical properties of the related zeolites offretite and erionite. *American Mineral* 54:875–86.

Stanton, M. F., M. Layard, A. Tegeris, E. Miller, M. May, E. Morgan, and A. Smith. 1981. Relation of particles dimension to carcinogenicity in amphibole asbestoses and other fibrous minerals. *Journal Natural Cancer Institute* 67:965–75.

Staples, L. W., and J. A. Gard. 1959. The fibrous zeolite erionite: Its occurrence, unit cell, and structure. *MineralMag* 322:261–81.

Sweatman, T. R., and J. V. P. Long. 1969. Quantitative electron-probe microanalysis of rock-forming minerals. *Journal of Petrology* 10:332–79. doi:10.1093/petrology/10.2.332.

Temel, A., and M. N. Gündogdu. 1996. Zeolite occurrences and the erionite-mesothelioma relationship in Cappadocia, Central Anatolia, Turkey. *Mineralium Deposita* 31:539–47. doi:10.1007/BF00196134.

Van Gosen, B. S., T. A. Blitz, G. S. Plumlee, G. P. Meeker, and M. P. Pierson. 2013. Geologic occurrences of erionite in the United States: An emerging national public health concern for respiratory disease. *Environ Geochem Health* 35:419–30. doi:10.1007/s10653-012-9504-9.

Vignaroli, G., P. Ballirano, G. Belardi, and F. Rossetti. 2014. Asbestos fibre identification vs. evaluation of asbestos hazard in ophiolitic rock mélanges, a case study from the Ligurian Alps (Italy). *Environment Earth Sciences* 72:3679–98. doi:10.1007/s12665-014-3303-9.

Wagner, J. C., J. W. Skidmore, R. J. Hill, and D. M. Griffiths. 1985. Erionite exposure and mesotheliomas in rats. *Br J Cancer* 51:727–30. doi:10.1038/bjc.1985.108.

Wise, W. S., and R. W. Tschernich. 1976. The chemical compositions and origin of the zeolites offretite, erionite and levyne. *American Mineral* 61:853–63.

Wiseman, H., and B. Halliwell. 1996. Damage to DNA by reactive oxygen and nitrogen species: Role in inflammatory disease and progression to cancer. *The Biochemical Journal* 313:17–29. doi:10.1042/bj3130017.

Wylie, A. G., and P. A. Candela. 2015. Methodologies for determining the sources, characteristics, distribution, and abundance of asbestiform and nonasbestiform amphibole and serpentine in ambient air and water. *Journal of Toxicology and Environmental Health, Part B* 18:1–42. doi:10.1080/10937404.2014.997945.

Young, R. A. 1993. *Introduction to the Rietveld method: In Young RA (ed) The Rietveld method*, 1–38. Oxford.

Zebedeo, C. N., C. Davis, C. Peña, K. W. Ng, and J. C. Pfau. 2014. Erionite induces production of autoantibodies and IL-17 in C57BL/6 mice. *Toxicology and Applied Pharmacology* 275:257–64. doi:10.1016/j.taap.2014.01.018.